Integrating TDD Communication and Radar Sensing in Co-Located Planar Array: A Genetic Algorithm Enabled Aperture Design

Hadi Alidoustaghdam*, Yang Miao and André Kokkeler
Radio Systems group, Faculty of Electrical Engineering, University of Twente
Enschede, the Netherlands
*: *hadi.alidoustaghdam@utwente.nl*

2022 2nd IEEE International Symposium on Joint Communications & Sensing (JC&S) | 978-1-6654-0579-9/22/$31.00 ©2022 IEEE | DOI: 10.1109/JCS54387.2022.9743500

***Abstract*—In this paper, we design interleaved transmitter (Tx) and receiver (Rx) apertures co-located in one planar array for enabling joint communication and sensing. A fixed number of antennas in a rectangular configuration is allocable for the apertures, and we use a genetic algorithm to determine the allocation. We assume that the Tx aperture transmits one beam to an active communication user (downlink communication of time division duplex) and another beam for sensing the passive target, and the Rx aperture receives backscattered sensing signals simultaneously (full duplex). The array apertures' design criteria are based on the effect of interference mitigation when using linear beamforming. The optimal solution is determined when the side lobes for the beams are minimized at different scanning angles in the field of view. Our numerical results indicate that the near-optimal antenna allocation for the apertures does not perform uniformly for all desired beam directions, but yet, we could conclude a near-optimal solution based on the least discrepancy between the sidelobe suppression effects for the aperture patterns.**

***Index Terms*—6G, joint communication and sensing, planar array apertures, interference mitigation.**

I. Introduction

The evolution toward 6G is featured by joint communication and sensing (JCAS) [1], [2]. To leverage advanced communication capabilities for sensing and to integrate innovative sensing into communication systems, fundamental changes to communication systems are required, both in hardware (transceiver, antenna array, etc.) design [3] and signal processing [4], wherein the antenna array geometry/configuration is crucial for the spatial resolution of radio signals and hence the performance of both sensing [5] and communication [6].

978-1-6654-0579-9/22/$31.00

Due to the long communication frames and the necessity for a perpetual sensing of the surrounding environment, in-band full-duplex (FD) JCAS is proposed [7] where communication and sensing operate simultaneously. In a simplified scenario, a transmitter (Tx) aperture generates two beams toward a communication user and a sensing target, whilst a receiver (Rx) aperture has a single beam toward the sensing target. The radiation patterns of the Tx and Rx apertures, when linear beamforming is adopted while guaranteeing the minimum interference among the patterns, rely on the geometries of arrays. It is discussed in [7] that the uniform linear co-located Tx and Rx apertures suffer from undesired mirror beams. A random displacement of array elements suppresses these mirror beams.

Designing proper co-located apertures for the transmitter and receiver does not only influence the performance of JCAS but also ensures an efficient spatial usage, e.g., the interleaved shared apertures. The shared aperture designs have been discussed in [8]–[10]. The intertwined Tx subarrays for dual function of radar and communication have been studied in [8] where the problem is formulated for a linear array design via convex optimization. In [9], designing sparse subarrays for multitask receivers has been investigated also via convex optimization.

Beyond the above-mentioned literature, this paper investigates the allocation of a limited number of antennas in a rectangular planar array for forming communication and sensing beams in various 3D directions in its field of view. The null-space pro-

jection matrix is used to guarantee the minimum interference between the Tx/Rx apertures. As a first step, the performance metrics for both communication and sensing are the side lobe level suppression in Tx/Rx aperture patterns. Considering the inherent non-convexity of the optimization problem, a genetic algorithm (GA) is used, where the GA has been customized for array topology design [11], array thinning [12] and also shared aperture design for a dual-band radar [10].

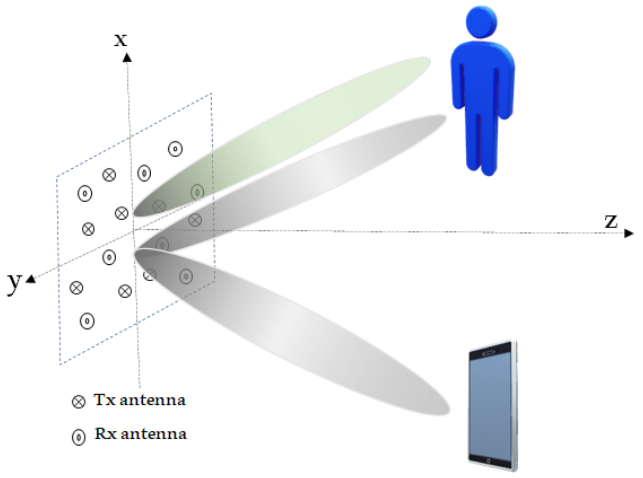

Fig. 1. A planar rectangular array with part of antennas for transmitting toward the communication user and the sensing target, and the other antennas for receiving from the sensing target.

II. Formulation of Problem

Let us consider a scenario as in Fig. 1 where $N_x \times N_y$ antenna elements in a rectangular planar array are divided, possibly non-uniformly, for the Tx and Rx apertures. The Tx aperture with N_{Tx} antennas generates one beam toward the communication user and another beam toward the sensing target, whereas the Rx aperture with N_{Rx} antennas has a single beam scanning for sensing signals. The beam steering vector [13] for a phased array with N isotropic antennas is defined as:

$$\mathbf{a}(\phi,\theta) = \left[e^{j\beta(x_1 u + y_1 v)}, ..., e^{j\beta(x_N u + y_N v)}\right]^T, \quad (1)$$

where $u = \cos\phi\sin\theta$, $v = \sin\phi\sin\theta$ in which ϕ and θ are the azimuth and co-elevation angles respectively in the local coordinate of the array whose origin is at the array center as is shown in Fig. 1; the angles denote the desired beam focusing direction. x_i and y_i in (1) are the coordinates of the ith antenna. Assuming narrowband beamforming, β denotes the wave-number at the center frequency of antennas.

Using linear beamforming, the weights for the antennas $\mathbf{w}_t$ at the Tx aperture can be obtained by:

$$\mathbf{w}_t = \frac{\left(\sqrt{\rho}\mathbf{a}_t(\phi_c,\theta_c) + \sqrt{1-\rho}\mathbf{a}_t(\phi_r,\theta_r)\right)^*}{\left\|\sqrt{\rho}\mathbf{a}_t(\phi_c,\theta_c) + \sqrt{1-\rho}\mathbf{a}_t(\phi_r,\theta_r)\right\|}, \quad (2)$$

where $\mathbf{a}_t$ denotes the steering vector of Tx aperture, $\zeta_c = (\phi_c,\theta_c)$ is the direction towards the communication user and $\zeta_r = (\phi_r,\theta_r)$ is the direction towards the sensing target, which are estimated beforehand. The power allocation between the communication beam and sensing beam is controlled by $0 < \rho < 1$ which is chosen 0.5 here. The radiated power from the Tx aperture is:

$$D_{\text{Tx}}^{\zeta_c,\zeta_r}(\phi,\theta) = 20\log_{10}\left|\mathbf{a}_t(\phi,\theta)^T\mathbf{w}_t\right|. \quad (3)$$

In order to mitigate the mutual interference and nullify the received reflected power from the communication user, one can combine the null space projection matrix and linear beamforming for calculating the weights $\mathbf{w}_r$ for the Rx aperture as [7]:

$$\mathbf{w}_r = \frac{\left((\mathbf{I}-\mathbf{F}\mathbf{F}^\dagger)\mathbf{a}_r(\phi_r,\theta_r)\right)^*}{\left\|(\mathbf{I}-\mathbf{F}\mathbf{F}^\dagger)\mathbf{a}_r(\phi_r,\theta_r)\right\|}, \quad (4)$$

where $\mathbf{I}$ is the identity matrix, $\mathbf{F} = [\mathbf{H}_{\text{SI}}\mathbf{w}_t^T, \mathbf{a}_r(\phi_c,\theta_c)]$, $\mathbf{F}^\dagger$ is the pseudo-inverse for $\mathbf{F}$, $\mathbf{H}_{\text{SI}} \in \mathbb{C}^{N_{Rx}\times N_{Tx}}$ denotes the inherent coupling from Tx antennas to Rx antennas which can be obtained by combination of electromagnetic simulations and mathematical calculation as in [6], [14], [15], besides $\mathbf{a}_r(\phi_c,\theta_c)$ and $\mathbf{a}_r(\phi_r,\theta_r)$ are the beam steering vectors in the Rx aperture toward the communication user and the sensing target, respectively. The received power from the Rx aperture by using linear beamforming is:

$$D_{\text{Rx}}^{\zeta_c,\zeta_r}(\phi,\theta) = 20\log_{10}\left|\mathbf{a}_r(\phi,\theta)^T\mathbf{w}_r\right|. \quad (5)$$

A. Optimization by Genetic Algorithm

A binary genetic algorithm [12] will be employed for dividing antenna elements between Tx and Rx apertures. To decrease the complexity, we consider a symmetric design where only the antennas at the first quarter of the rectangular array are the optimization variables and the other quarters are its mirrored replica. In total, N_g matrices of $\mathbf{B} \in$

$\mathbb{N}^{N_x/4\times N_y/4}$ are generated where the elements in $\mathbf{B}$ are chosen randomly from binary numbers, with the ones $\mathbf{1}$ denoting the antennas are allocated for the Tx aperture and the zeros $\mathbf{0}$ denote allocation for the Rx aperture. The weights of antennas and radiation patterns for the Tx and Rx apertures are obtained by (2)-(5). The cost function is defined based on the level of side lobes in (6), where k denotes an index for the matrix $\mathbf{B}$ where $1 \leq k \leq N_g$. The angles for beams of communication and sensing are one angular resolution of this rectangular aperture. We consider only high side lobe levels, so $\zeta_{sl,\text{Tx}}$ and $\zeta_{sl,\text{Rx}}$ are the angles for the side lobes sl where $\max(D^{k,\zeta_c,\zeta_r}_{\text{Tx or Rx}}) - D^{k,\zeta_c,\zeta_r}_{\text{Tx or Rx}}(\zeta_{sl,\text{Tx or Rx}}) < 25$ dB, this appoints only those angles in which the difference of power in side lobe and maximum gain is less than 25 dB, so $n_{\zeta_{sl,\text{Tx}}}$ and $n_{\zeta_{sl,\text{Rx}}}$ denote the numbers of side lobe angles with the above condition for Tx and Rx patterns, respectively. The average of side lobe levels for the Tx and Rx patterns are denoted by $\mathrm{S}^{k,\zeta_c,\zeta_r}_{sl,\text{Tx}}$ and $\mathrm{S}^{k,\zeta_c,\zeta_r}_{sl,\text{Rx}}$. Besides, n_{ζ_c} and n_{ζ_r} are the numbers of scanning angles for the communication user and the sensing target, respectively, and $f(k)$ is the cost function to be maximized.

$$
\begin{aligned}
\mathrm{S}^{k,\zeta_c,\zeta_r}_{sl,\text{Tx}} &= \frac{\sum_{\zeta_{sl,\text{Tx}}} \left(\max(D^{k,\zeta_c,\zeta_r}_{\text{Tx}}) - D^{k,\zeta_c,\zeta_r}_{\text{Tx}}(\zeta_{sl,\text{Tx}})\right)}{n_{\zeta_{sl,\text{Tx}}}}, \\
\mathrm{S}^{k,\zeta_c,\zeta_r}_{sl,\text{Rx}} &= \frac{\sum_{\zeta_{sl,\text{Rx}}} \left(\max(D^{k,\zeta_c,\zeta_r}_{\text{Rx}}) - D^{k,\zeta_c,\zeta_r}_{\text{Rx}}(\zeta_{sl,\text{Rx}})\right)}{n_{\zeta_{sl,\text{Rx}}}}, \\
\mathrm{S}^{k,\zeta_c,\zeta_r}_{sl} &= 0.5 \times \mathrm{S}^{k,\zeta_c,\zeta_r}_{sl,\text{Tx}} + 0.5 \times \mathrm{S}^{k,\zeta_c,\zeta_r}_{sl,\text{Rx}}, \\
f(k) &= \frac{\sum_{\zeta_c}\sum_{\zeta_r} \mathrm{S}^{k,\zeta_c,\zeta_r}_{sl}}{n_{\zeta_c} n_{\zeta_r}},
\end{aligned}
\tag{6}
$$

At each iteration, the cost functions for all matrices of $\mathbf{B}$ are calculated and the gene with the highest $f(k)$ is compared with the best global solution. Then, half of the genes with smaller values of $f(k)$ are discarded and replaced with the genes with larger values of $f(k)$. A random horizontal row in $\mathbf{B}$ is considered for the line cross-over of parents, and bit flip mutation is applied on some candidates [11]. The algorithm iterates N_{it} times and $\max(f)$ is monitored to assure the convergence of optimization.

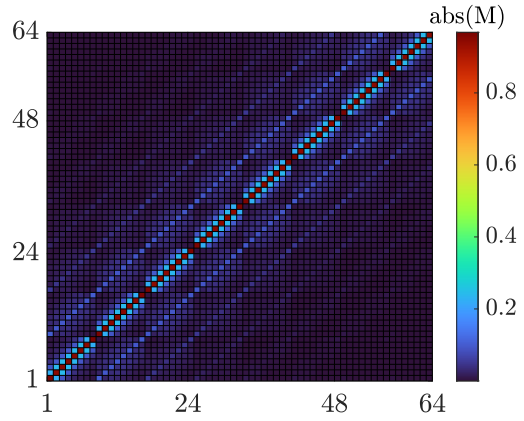

Fig. 2. The magnitude of mutual coupling of antenna elements.

B. Numerical Analysis

Let us consider each antenna element as a rectangular patch antenna with the patch size of $l_x \times l_y = 3.9 \times 2.73$ mm^2 on the Rogers RO3003 substrate with thickness 0.25 mm, relative permittivity of $\epsilon_r = 3$ and copper cladding thickness of 35 μm, which is designed for the center frequency of f_c =28 GHz, bandwidth of $\text{BW}_{10\text{ dB}} = 863$ MHz and half-power beamwidth of $89.3° < \theta_{3\text{ dB}} < 119.1°$ for various ϕs. A planar rectangular array with $N_x \times N_y = 8 \times 8$ patch antennas and inter-element spacing of $d_0 = \lambda_c/2$ is considered, where λ_c is the wavelength at the frequency f_c. The mutual couplings of antenna elements are calculated and recorded in the matrix $\mathbf{M} \in \mathbb{C}^{N_xN_y \times N_xN_y}$, which is shown in Fig. 2, by the methods in [6], [14], [15]. $\mathbf{H}_{\text{SI}}$ can be extracted from $\mathbf{M}$ based on the antennas, which are allocatable between Tx and Rx apertures. The smallest angular resolutions for the Tx and Rx apertures are $\delta_\theta = 1.22\lambda_c/d_x$ and $\delta_\phi = 1.22\lambda_c/d_y$ where $d_x = (N_x - 1)d_0$ is the length of aperture in x axis and $d_y = (N_y - 1)d_0$ is the length of aperture in y axis [5]. In order to expedite the optimization, the azimuth and elevation angles in (3) and (5) are swept with $\delta_\phi/2$ and $\delta_\theta/2$, respectively. Due to the symmetry, we select $0 < \phi_r < 90°$ with steps of $2\delta_\phi$ for the scanning angle of target which corresponds to only one quarter of such square aperture, whereas the angle of communication user will be $0 < \phi_c < 360°$ with steps of $2\delta_\phi$, besides $0 < \theta_r < 45°$, $0 < \theta_c < 45°$ with steps of $2\delta_\theta$. As the beamforming in (4) nullifies the receiving power

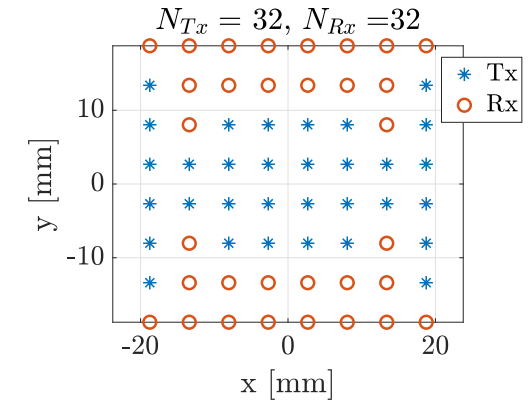

(a)

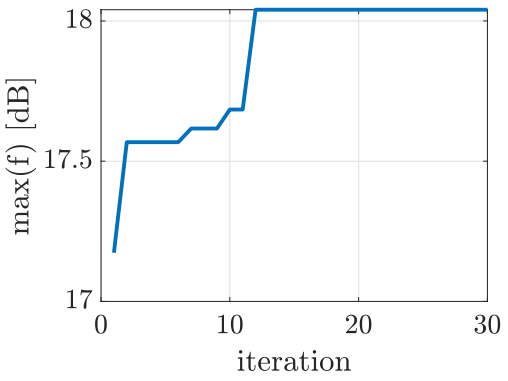

(b)

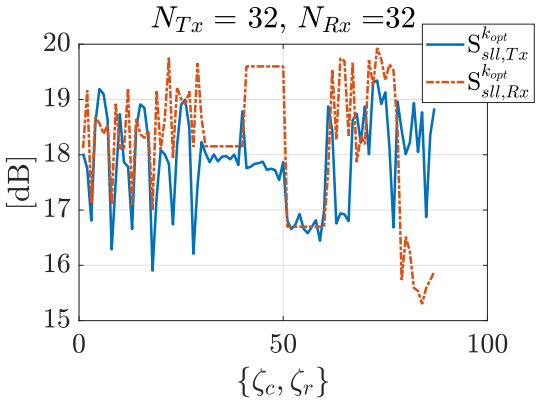

(c)

Fig. 3. (a) The optimized Tx and Rx apertures, (b) the convergence of GA and (c) the average of side lob levels of its radiation pattern where x-axis is the enumeration of $\{\zeta_c, \zeta_r\}$ pairs.

of the Rx aperture from the angle of the communication user, we do not consider the cases when $\zeta_c = \zeta_r$, in which the angles of the communication and sensing are overlapping. The number of genes N_g is chosen 60 which half of them are mutated with a rate of $\mu = 0.5$ at each iteration and the number of iterations is $N_{it} = 30$.

Fig. 3 (a) shows the resultant geometry after the optimization and Fig. 3 (b) indicates the convergence of max(f). In order to check the performance of this geometry, $S_{sl,\mathrm{Tx}}^{k_{\mathrm{opt}},\zeta_c,\zeta_r}$ and $S_{sl,\mathrm{Rx}}^{k_{\mathrm{opt}},\zeta_c,\zeta_r}$ which are the average of side lobe suppression for the optimum solution k_{opt}, are compared in different angles of $\{\zeta_c, \zeta_r\}$ pairs as in Fig. 3 (c). It is observed that the average side lobe levels in the patterns of Tx and Rx apertures depends on the scanning angles, besides, $S_{sl,\mathrm{Tx}}^{k_{\mathrm{opt}},\zeta_c,\zeta_r}$ and $S_{sl,\mathrm{Rx}}^{k_{\mathrm{opt}},\zeta_c,\zeta_r}$ are not equal. Let us demonstrate the Tx and Rx pattern for some angles as in Figs. 4 (a)-(b). It is observed that side lobe levels in the radiation pattern of the Tx aperture are lower than the side lobe levels of the Rx aperture, these high side lobe levels in the Rx pattern are detrimental for radar detections. The reason is that the weights of the antennas in the Rx aperture are constrained to cancel the interference in addition to beamforming toward the sensing target according to (4), which results in mirror beams for some angles as in the Rx patterns of Figs. 4 (a)-(b).

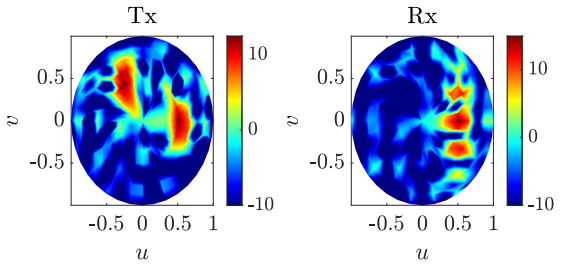

(a)

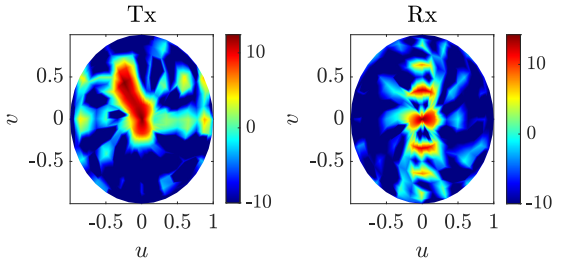

(b)

Fig. 4. The radiation patterns of optimized aperture for the angles (a) $(\phi_c, \theta_c) = (120°, 30°)$, $(\phi_r, \theta_r) = (90°, 30°)$ and (b) $(\phi_c, \theta_c) = (120°, 30°)$, $(\phi_r, \theta_r) = (0°, 0°)$. The colorbars are in dB.

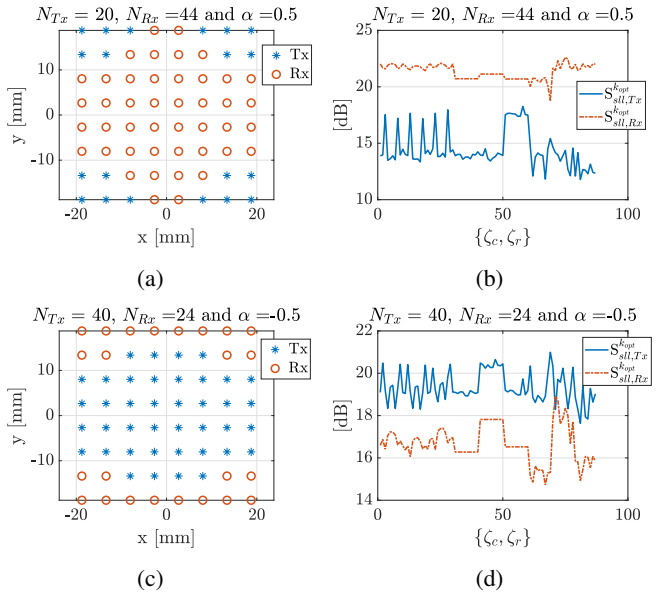

Fig. 5. The optimized geometry and its resultant average levels of side lobe suppression for (a) and (b) $\alpha = +0.5$, (c) and (d) $\alpha = -0.5$ besides, x-axes in (b) and (d) are the enumerations of $\{\zeta_c, \zeta_r\}$ pairs.

To control side lobe levels in the patterns of Rx aperture, one can add a tuning parameter $-1 < \alpha < 1$ to the $\mathrm{S}_{sl}^{k,\zeta_c,\zeta_r} = \frac{1-\alpha}{2}\mathrm{S}_{sl,\mathrm{Tx}}^{k,\zeta_c,\zeta_r} + \frac{1+\alpha}{2}\mathrm{S}_{sl,\mathrm{Rx}}^{k,\zeta_c,\zeta_r}$ which controls the average side lobe levels of Tx and Rx apertures. The optimum solutions are obtained for different αs and shown in Figs. 5 (a)-(d), when $\alpha = +0.5$ which resulted in $N_{Tx} = 20$ and $N_{Rx} = 44$, the Rx pattern has higher side lobe suppression as in Figs. 5 (b), however when $\alpha = -0.5$ which resulted in $N_{Tx} = 40$ and $N_{Rx} = 24$, the Tx pattern has higher side lobe suppression, therefore considering the communication and active sensing via this aperture, the case of $\alpha = 0$ which resulted in the equal antenna allocation $N_{Tx} = N_{Rx} = 32$ and fair average side lobe suppression ($|\mathrm{S}_{sl,\mathrm{Tx}}^{k_{opt},\zeta_c,\zeta_r} - \mathrm{S}_{sl,\mathrm{Rx}}^{k_{opt},\zeta_c,\zeta_r}| < 3$ dB) as in Fig. 3 (c), is still the best choice.

III. Conclusion

In this paper, the interleaved transmit and receive apertures are designed for integrating communication and sensing functionalities. With the assumptions of fixed number of antenna elements and fixed aperture size of a planar array, a genetic algorithm is used to determine a near-optimal global allocation of antennas, to mitigate interference between the transmitting communication and sensing beams, and the receiving focusing direction (beam).

In the numerical results, we showed that the side lobe suppression of Rx beam pattern can be outweighed to Tx beams' patterns through a tuning parameter, however the scenario of TDD communication and fullduplex sensing needs an equal side lobe suppression for both apertures. Wherein, the case when $N_{Tx} = N_{Rx} = 32$ has the best performance since the maximum difference of the average side lobe suppression between the Tx and Rx apertures' patterns is only 3 dB. Besides, the average sidelobe suppression (in power levels) of this geometry differs for different beam focusing directions, varying from 15.5 dB to 20 dB.

References

[1] C. De Lima and et al., "Convergent communication, sensing and localization in 6g systems: An overview of technologies, opportunities and challenges," *IEEE Access*, vol. 9, pp. 26 902–26 925, 2021.

[2] T. Wild, V. Braun, and H. Viswanathan, "Joint design of communication and sensing for beyond 5g and 6g systems," *IEEE Access*, vol. 9, pp. 30 845–30 857, 2021.

[3] J. Moghaddasi and K. Wu, "Multifunctional transceiver for future radar sensing and radio communicating data-fusion platform," *IEEE access*, vol. 4, pp. 818–838, 2016.

[4] J. A. Zhang, F. Liu, C. Masouros, R. W. Heath Jr, Z. Feng, L. Zheng, and A. Petropulu, "An overview of signal processing techniques for joint communication and radar sensing," *arXiv preprint arXiv:2102.12780*, 2021.

[5] A. Di Serio, P. Hügler, F. Roos, and C. Waldschmidt, "2-d mimo radar: A method for array performance assessment and design of a planar antenna array," *IEEE Transactions on Antennas and Propagation*, vol. 68, no. 6, pp. 4604–4616, 2020.

[6] X. Ge, R. Zi, H. Wang, J. Zhang, and M. Jo, "Multi-user massive mimo communication systems based on irregular antenna arrays," *IEEE Transactions on Wireless Communications*, vol. 15, no. 8, pp. 5287–5301, 2016.

[7] M. Heino, C. B. Barneto, T. Riihonen, and M. Valkama, "Design of phased array architectures for full-duplex joint communications and sensing," in *2021 15th European Conference on Antennas and Propagation (EuCAP)*. IEEE, 2021, pp. 1–5.

[8] X. Wang, A. Hassanien, and M. G. Amin, "Sparse transmit array design for dual-function radar communications by antenna selection," *Digital Signal Processing*, vol. 83, pp. 223–234, 2018.

[9] A. Deligiannis, M. Amin, S. Lambotharan, and G. Fabrizio, "Optimum sparse subarray design for multitask receivers," *IEEE Transactions on Aerospace and Electronic Systems*, vol. 55, no. 2, pp. 939–950, 2018.

[10] G. Kwon, J. Park, D. Kim, and K. C. Hwang, "Optimization of a shared-aperture dual-band transmitting/receiving array antenna for radar applications," *IEEE Transactions on Antennas and Propagation*, vol. 65, no. 12, pp. 7038–7051, 2017.

[11] K. Shen, T. De Pessemier, L. Martens, W. Joseph, and Y. Miao, "Genetic algorithm combined with ray tracer for optimizing cell-free mmimo topology in a confined environment," in *2021 15th European Conference on Antennas and Propagation (EuCAP)*, 2021, pp. 1–5.

[12] R. L. Haupt, "Thinned arrays using genetic algorithms," *IEEE Transactions on Antennas and Propagation*, vol. 42, no. 7, pp. 993–999, 1994.

[13] Y. Miao, W. Fan, J. Takada, R. He, X. Yin, M. Yang, J. Rodríguez-Piñeiro, A. A. Glazunov, W. Wang, and Y. Gong, "Comparing channel emulation algorithms by using plane waves and spherical vector waves in multiprobe anechoic chamber setups," *IEEE Transactions on Antennas and Propagation*, vol. 67, no. 6, pp. 4091–4103, 2019.

[14] Y. Sun, Y. Chow, and D. Fang, "Mutual impedance formula between patch antennas based on synthetic asymptote and variable separation," *Microwave and Optical Technology Letters*, vol. 35, no. 6, pp. 466–470, 2002.

[15] D. R. Jackson, W. F. Richards, and A. Ali-Khan, "Series expansions for the mutual coupling in microstrip patch arrays," *IEEE transactions on antennas and propagation*, vol. 37, no. 3, pp. 269–274, 1989.